

**HHS PUBLIC ACCESS**

Author manuscript

Nanoscale. Author manuscript; available in PMC 2017 April 28.

Published in final edited form as:

Nanoscale. 2016 April 28; 8(17): 9178–9184. doi:10.1039/c5nr08895j.

Endosome-Mimicking Nanogels for Targeted Drug Delivery**Jicheng Yu^{a,b}, Yuqi Zhang^{a,b}, Wujin Sun^{a,b}, Chao Wang^{a,b}, Davis Ranson^a, Yanqi Ye^{a,b}, Yuyan Weng^c, and Zhen Gu^{a,b,d}**Yuyan Weng: wengyy@suda.edu.cn; Zhen Gu: zgu@email.unc.edu^aJoint Department of Biomedical Engineering, University of North Carolina at Chapel Hill and North Carolina State University, Raleigh, NC 27695, USA^bMolecular Pharmaceutics Division, Eshelman School of Pharmacy, University of North Carolina at Chapel Hill, Chapel Hill, NC 27599, USA^cCenter for Soft Condensed Matter Physics and Interdisciplinary Research & College of Physics, Optoelectronics and Energy, Soochow University, Suzhou, 215006, China^dDepartment of Medicine, University of North Carolina School of Medicine, Chapel Hill, NC 27599, USA**Abstract**

Drug delivery systems inspired by natural particulates hold great promise for targeted cancer therapy. Endosome formed by internalization of plasma membrane has massive of membrane proteins and receptors on the surface, which is able to specifically target to the homotypic cells. Herein, we describe a simple method to fabricate an endosome membrane-coated nanogel (EM-NG) from source cancer cells. Following intracellular uptake of methacrylated hyaluronic acid (*m*-HA) adsorbed SiO₂/Fe₃O₄ nanoparticles encapsulating crosslinker and photoinitiator, EM-NG was readily prepared through *in situ* crosslinking initiated under UV irradiation inside endosome. The resulting endosome mimetic nanogels loaded with Doxorubicin (DOX) displayed enhanced internalization efficiency to the source cells through a specific homotypic affinity *in vitro*. However, when treated the non-source cells, the EM-NGs exhibited insignificant difference in therapeutic efficiency compared to bare HA nanogel with DOX. This study illustrates the potential of utilizing endosome membrane-mimicking formulation for targeted cancer therapy, and offers guideline for developing natural particulates-inspired drug delivery system.

Introduction

Drug delivery systems based on natural particulates have emerged as one of the most promising strategies for cancer therapy¹. Taking advantages of physical morphologies and biological functions of natural particulates, these biomimetic drug delivery carriers offer several significant advantages such as selective targeting, prolonged circulation time, and low immunogenicity^{2–6}. Among them, natural biological membrane-derived nanoparticles

Correspondence to: Yuyan Weng, wengyy@suda.edu.cn; Zhen Gu, zgu@email.unc.edu.

[†]Electronic supplementary information (ESI) available: Synthesis of *m*-HA; Synthesis of rhodamine-HA derivative; supplementary data on relative fluorescence intensity of DOX-EN-NGs on HeLa cells. See DOI:

(NPs) have received extensive attention as a simple and viable manner due to their capability of mimicking the natural membrane properties. For example, red blood cell membrane-coated PLGA nanoparticles have shown superior circulation half-life *in vivo*⁷⁻¹⁰. In addition, it has been validated that cancer cell membrane-coated nanoparticles with full array of tumor antigens can promote a tumor-specific immune response and target to the source cancer cells *via* an inherent homotypic binding interaction¹¹. Our previously reported work demonstrated that the platelet membrane coated core-shell nanovehicle with overexpressed P-Selectin on the membrane could specifically bind to CD44 receptors on the surface of cancer cells¹².

Endosome plays an important role in regulating fundamental processes in eukaryotic cells, such as nutrient uptake, signaling, immunity and adhesion¹³. The massive amount of membrane is internalized into endosome by several endocytic pathways, and the membrane lipids and proteins can be recycled back to the plasma membrane in an efficient manner¹³⁻¹⁵. Although precise mechanisms of the recycling and fusion remain to be fully elucidated, several previous studies revealed endosome-to-plasma membrane transport is mediated with several proteins including Eps15p homology (EH) domains containing proteins^{16, 17}. The proteins from the sorting nexin protein family and others can also promote the fusion of endosome with the plasma membrane¹⁸⁻²¹.

In this study, we describe an endosome membrane-coated nanogel (denoted as EM-NG) which is easily extracted from the source cancer cells for targeting and specific delivery of small molecular drug. As shown in Fig. 1, the EM-NG has an inner core composed of hyaluronic acid (HA) nanogel containing SiO₂/Fe₃O₄ nanoparticles, and an endosome membrane based outer shell. HA is chosen since it is highly biocompatible and it can target to the hyaluronan receptors CD44, which are overexpressed in a variety of tumor types²²⁻²⁶. In order to allow HA nanogel form inside endosome directly, we firstly use core-shell mesoporous silica NPs with Fe₃O₄ nanocrystals as the core (SiO₂/Fe₃O₄ NPs) to encapsulate crosslinker and photoinitiator, and coat with methacrylated HA (*m*-HA) on the surface through electrostatic interaction. Following the incubation of resulting NPs with source cells, an *in situ* formed nanogel in endosome is obtained by the photo-polymerization upon UV light irradiation²⁷⁻³². The endosome containing HA nanogel is readily collected *via* the magnetic extraction due to the entrapped magnetic Fe₃O₄ nanocrystals. After loading with anticancer drug Doxorubicin (DOX), these EM-NGs can actively target to source cancer cells by taking the advantage of the specific interaction with their source cells, and subsequently internalize to release DOX.

Experimental

Materials

All chemicals were purchase from Sigma-Aldrich and were used as received. Rhoadmine-NHS was purchase from Life Technologies (Grand Island, NY, USA).

Synthesis of Fe₃O₄ nanocrystals

A solution of 1 M iron (III) chloride hexahydrate and 0.5 M iron (II) chloride tetrahydrate in 25 mL DI water was added dropwise to a 0.5 M NaOH solution in 250 mL of DI water at 40°C. The mixture was stirred for 1 h and the nanocrystals subsequently washed with DI water until pH neutral. The resulting nanocrystals were dialyzed against DI water for 3 days. Finally, the Fe₃O₄ nanocrystals were stabilized with oleic acid and dispersed in chloroform with a concentration of 6.7 mg Fe/mL. The zeta-potential and size distribution were measured on the Zetasizer (Nano ZS; Malvern). The TEM images were obtained on a JEOL 2000FX TEM instrument.

Synthesis of SiO₂/Fe₃O₄ NPs functionalized with quaternary ammonium groups

1 mL of the Fe₃O₄ nanocrystals in chloroform was poured into 10 mL of 0.55M aqueous cetyltrimethylammonium bromide (CTAB) solution and emulsified by sonication for 10 min. The resulting turbid brown solution was stirred and heated up to 65 °C for 10 min to evaporate the chloroform, resulting in a transparent black Fe₃O₄/CTAB solution. Then, the Fe₃O₄/CTAB solution was added to a mixture of 90 mL of water and 0.6 mL of 2N NaOH solution, and the mixture was heated up to 70 °C under stirring. After adding 1 mL of tetraethylorthosilicate (TEOS) and 6 mL of ethylacetate, the solution was stirred at 70 °C for 3 h. Thereafter, the obtained SiO₂/Fe₃O₄ NPs were washed 3 times with ethanol to remove the unreacted species and dispersed in 30 mL of ethanol. To extract CTAB, 80 μL of HCl was added to the solution and stirred for 3 h at 60 °C. After washing them with ethanol three times, the NPs were dispersed in 10 mL of chloroform, and 120 μL of 3-trimethoxysilylpropyl-*N,N,N*-trimethylammonium chloride (TMAPS) 50% in methanol was added. The reaction solution was stirred at room temperature for 24 h. The resulting SiO₂/Fe₃O₄ NPs functionalized with quaternary ammonium groups were wash 3 times with ethanol and dried in vacuum.

Preparation of HA/SiO₂/Fe₃O₄ NPs

3 mg SiO₂/Fe₃O₄ NPs was mixed with 0.5 mg *N,N'*-methylenebisacrylamide (MBA) and 0.1 mg photoinitiator (Irgacure 2959) in PBS buffer for 24 h. Unloaded crosslinker and photoinitiator was removed by filtering using a centrifugal filter (100,000 Da molecular mass cutoff, Millipore). Then, 1 mg *m*-HA or rhodamine-HA derivative was added and stirred for another 4 h to obtain HA/SiO₂/Fe₃O₄ NPs.

Cell culture

HeLa and A549 cells were obtained from Tissue Culture Facility of UNC Lineberger Comprehensive Cancer Center and cultured in Dulbecco's Modified Eagle's Medium supplemented with 10% (v/v) fetal bovine serum (FBS), penicillin (100 U/mL) and streptomycin (100 μg/mL) in a 37°C incubator (Thermal Scientific) under 5% CO₂ and 90% humidity. The cells were regularly sub-cultured with trypsin-EDTA (0.25%, w/w) and cell density was determined with hemocytometer before each experiment.

Preparation of EM-NG and HA NG

HeLa cells (1×10^5 cells per well) were seeded in 6-well plates. The cells were allowed to culture for 24 h before exposure to the HA/SiO₂/Fe₃O₄ NPs dispersions. The NPs dispersions were prepared by diluting the concentrated NPs solution into the FBS free medium. The cells were incubated with NPs for 4 h, then the NPs containing medium was discarded. After washing the cells by PBS twice, the cells were harvested with trypsin and centrifuged at 1000 rpm for 4 min. Then, the cells were resuspended in 1 mL PBS solution and exposed to UV irradiation (wavelength: 365 nm) for 1 min to form solid HA nanogel by crosslinking polymerization. The cells were lysed with Pierce IP lysis buffer (Thermo Scientific). Then, EM-NGs were collected using a magnet from the cells lysate. In order to obtain the bare HA nanogel without endosome membrane, the EM-NG were further lysed with lysis buffer for a second time, and collected using a magnet.

Intracellular distribution of HA/SiO₂/Fe₃O₄ NPs

HeLa cells (1×10^5 cells per dish) were seeded in confocal dishes and cultured for 24 h. Then, the cells were incubated with rhodamine-HA/SiO₂/Fe₃O₄ NPs for 1 h and 4 h. Afterward, the cells were washed with PBS twice and stained by LysoTracker green (50 nM) (Life Technologies) at 37°C for 30 min. Then, the cells were washed with PBS twice and stained with Hoechst 33342 (1 µg/mL) for 10 min. After washing with PBS twice, the cells were immediately observed using CLSM (LCM 710, Zeiss).

Preparation of DOX-EM-NG

To prepare DOX-EM-NG, 0.03 mL of DOX solution (0.1 mg/mL) was added into 0.27 mL of EM-NG solution, and mixed at room temperature for 24 h. Then, the excess DOX was removed by filtering using a centrifugal filter (10,000 Da molecular mass cutoff, Millipore). The loading capacity (LC) of DOX-EM-NG were determined by measuring the amount of encapsulated DOX by analyzing fluorescence intensity of DOX at 590 nm with an excitation wavelength of 480 nm using microplate reader (Infinite M200 Pro, Tecan). LC was calculated as LC=encapsulated amount of DOX/total weight of DOX-EM-NGs.

Endosome membrane protein characterization

SDS-PAGE was used to separate the proteins contained in the endosome only, EM-NGs and NGs. Samples were diluted in protein loading buffer and incubated for 10 min at 100°C. 10 µL of sample was loaded into each well in a 10% polyacrylamide gel. After separation by SDS-PAGE, the proteins were transferred to a nitro cellulose membrane at 300 mA for 3 h using a wet transfer method. The membrane was incubated with a 3% BSA blocking solution in the PBS TWEEN solution (0.01%) for 30 min at room temperature, and then incubated with early endosome antigen 1 (EEA1) in blocking solution overnight at 4°C. Afterward, the membrane was washed 3 times with PBS TWEEN 0.01% and incubated with the anti-rabbit HRP in blocking solution for 1 h. The membrane was then washed with PBS TWEEN 0.01% for 3 times and visualized using a 1-Step™ TMB-Blotting solution (Pierce, USA).

***In vitro* DOX release study**

The release profile of DOX was measured using dialysis method in PBS buffer. 400 μL of DOX-EM-NG solution was added into a dialysis tube (10,000 Da molecular mass cutoff) (Slide-A-Lyzer, Thermo Scientific) against 1 mL of PBS buffer solution with different pH (7.4 and 5.0). The dialysis tube was incubated at 37°C. At predetermined time intervals, the total buffer solution was withdrawn, followed by replacing with fresh buffer solution with the same pH. The amount of release DOX was measured through the same method mentioned above.

Determination of endocytosis pathways

HeLa cells (1×10^5 cells per well) were seeded in 6-well plates and cultured for 48 h. Afterwards, the cells were pre-incubated with different specific inhibitors for different endocytosis pathways, including chlorpromazine (CPZ, 10 μM) for the clathrin-mediated endocytosis, nystatin (NYS, 25 $\mu\text{g}/\text{mL}$) for the caveolin-mediated endocytosis inhibition, amiloride (AMI, 1 mM) for the macropinocytosis inhibition, and methyl- β -cyclodextrin (MCD, 3 mM) for the lipid raft inhibition. Then, the cells were incubated with DOX-EM-NG at DOX concentration of 1 μM in the presence of the inhibitors for another 2 h. After washing the cells by 4°C PBS twice, the fluorescence intensity of DOX in the cells were measured by the flow cytometry.

Evaluation of DOX-EM-NG and DOX-NG uptake of HeLa cells

HeLa cells (1×10^5 cells per well) were seeded in 6-well plates and cultured for 48 h. Afterwards, the cells was added with DOX-EM-NGs, DOX-NGs, and free DOX with same concentration, and incubated for 2 h. After washing the cells by 4 °C PBS twice, the fluorescence intensity of DOX in the cells were measured by the flow cytometry.

***In vitro* cytotoxicity**

HeLa or A549 cells (6×10^3 cells per well) were seeded in the 96-well plates. After 24 h culture, the cells were exposed to EM-NGs, free DOX solution, DOX-EM-NGs and DOX-NGs with different concentrations of DOX in FBS free medium for 24 h, respectively. Then, 20 μL per well of MTT solution (5 mg/mL) was added and incubated for another 4 h. After removing the medium, 150 μL DMSO was added to each well. The absorbance was measured at a test wavelength of 570 nm with a reference wavelength of 630 nm by a microplate reader (Infinite M200 PRO, Tecan).

Statistical analysis

All results presented are Mean \pm SEM. Statistical analysis was performed using Student's *t*-test or ANOVA test. With a *p* value < 0.05, the differences between experimental groups and control groups were considered statistically significant.

Results and discussion

Preparation and characterization of HA/SiO₂/Fe₃O₄ NPs

Magnetic Fe₃O₄ nanocrystals was synthesized by a traditional aqueous co-precipitation technique³³. The obtained Fe₃O₄ nanocrystals was characterized by dynamic light scattering (DLS) and transmission electron microscope (TEM). As shown in Fig. 2a and b, the Fe₃O₄ nanocrystals were monodispersed with an average diameter of 22.5 nm. These nanocrystals were then coated with mesoporous silica using a sol-gel method³⁴. DLS results revealed that the size of SiO₂/Fe₃O₄ NPs increased to 115.3 nm, and the wormhole-like mesopores with a size of about 2-3 nm were clearly observed in the silica shells in TEM image (Fig. 2c and d). The zeta potential of silica nanoparticles was determined as -30.1±3.3 mV due to surface hydroxyl groups.

To adsorb negatively charged *m*-HA on the surface, 3-trimethoxysilylpropyl-*N,N,N*-trimethylammonium chloride (TMAPS) was further functionalized with SiO₂/Fe₃O₄ NPs to provide quaternary ammonium groups on the outer surface, which converted the zeta potential to 23.2±0.4 mV. After loaded with crosslinker and photoinitiator, *m*-HA was subsequently deposited onto the positively charged SiO₂/Fe₃O₄ NPs by the electrostatic assembly. The TEM image clearly showed the HA shell on the surface of SiO₂/Fe₃O₄ NPs (Fig. 2e). The negative zeta potential of obtained HA/SiO₂/Fe₃O₄ NPs (-36±1.5 mV) and an apparent increase in diameter measured by DLS (Figure 2f) further validated the successful coating of *m*-HA on the surface of SiO₂/Fe₃O₄ NPs.

Preparation and characterization of EM-NGs

To achieve the endosome membrane coating HA nanogels, HA/SiO₂/Fe₃O₄ NPs were first required to interact with endosomes. Human cervical carcinoma epithelial (HeLa) cell was chosen as a model cell line, and HA/SiO₂/Fe₃O₄ NPs were incubated in the cell culture medium with cells. HA/SiO₂/Fe₃O₄ NPs was allowed to internalize the endosome *via* the endo-lysosomal pathway. The successful uptake of HA/SiO₂/Fe₃O₄ NPs in endosome was confirmed using the confocal laser scanning microscopy (CLSM). The fluorescence signal of the rhodamine tagged HA/SiO₂/Fe₃O₄ NPs was clearly observed in cells after 4 h of coincubation, and the fluorescence signals of rhodamine and LysoTracker Green showed high colocalization (Fig. 3a), suggesting most of HA/SiO₂/Fe₃O₄ NPs existed in the endosomes. After removing the free NPs, the cells were exposed to UV light to initiate the *in situ* photo-polymerization to form the crosslinked HA nanogel in the endosome, namely EM-NG. The cells were then lysed, and EM-NG containing magnetic nanoparticle were collected *via* magnetic extraction (Fig. 3d). As determined by DLS, the EM-NG was 262.3 nm in hydrodynamic diameter (Fig. 3c). The TEM picture showed the EM-NGs were round-oval in shape, and the membrane with a thickness of 10 nm and the multiple of inclusions of silica NPs were clearly observed in each EM-NG (Fig. 3b). To further confirm the successful coating of endosome membrane, the western blotting analysis was performed against the early endosome antigen 1 (EEA1), the endosome membrane-specific marker. The result showed a significant enrichment of EEA1 was present on the EM-NGs rather than the bare HA NGs (Fig. 3e).

Drug loading and release from EM-NGs

DOX, as a model hydrophilic anticancer drug, was loaded into EM-NG *via* dispersion^{35,36}. The loading capacity was determined as 7.3%. The *in vitro* drug release behavior was investigated under different pH conditions over time. The DOX-EM-NG exhibited near a zero-order release kinetics at pH 7.4 (Fig. 3f). In contrast, DOX released from nanogel was much faster at an acidic condition than physiological condition. The accelerated drug release at acidic pH is mainly due to the weakening of the binding between the EM-NG and drug, and improved solubility of DOX at low pH^{37,38}. This pH-dependent drug release behavior can play a crucial role in tumor-targeted drug delivery *via* endocytosis pathway.

In vitro delivery of DOX by EM-NG

In order to determine the endocytosis pathway of DOX-EM-NG, HeLa cells were pre-incubated with several specific inhibitors of different kinds of endocytosis, including chlorpromazine (CPZ) for clathrin-mediated endocytosis, nystatin (NYS) for the caveolin-mediated endocytosis inhibition, amiloride (AMI) for the macropinocytosis inhibition, and methyl- β -cyclodextrin (MCD) for the lipid raft inhibition. As shown in Fig. 4b, CPZ, NYS and AMI all reduced the uptake of DOX-EM-NG significantly, suggesting that DOX-EM-NG were taken up by HeLa cells through clathrin-mediated endocytosis, caveolin-mediated endocytosis, and lipid raft. In contrast, there was insignificant inhibition of uptake efficiency in the cells pretreated with AMI for the macropinocytosis inhibition. These results indicated that several pathways were involved in the internalization of cell membrane with DOX-EM-NG, due to a large number of receptors and proteins on the surface of endosome membrane shell of DOX-EM-NG^{13, 15}. The fluorescence of DOX was clearly observed in cells after 1 h of incubation with DOX-EM-NG, visualized by CLSM (Fig. 4a and Fig. S1 in the ESI[†]), which validated the cellular internalization of DOX-EM-NG. When prolonged the incubation time to 4 h, DOX was remarkably released and delivered into the nuclei of cells. To explore the targeting capability of DOX-EM-NG, EM-NG extracted from HeLa cells was further lysed to obtain the bare HA nanogel (NG) by removing the endosome membrane³⁹. By quantitative analysis using the flow cytometry, it was demonstrated that incubation of DOX-EM-NG with HeLa cells *in vitro* led to significantly increased uptake as compared to the DOX loaded bare HA nanogel (DOX-NG) and free DOX (Fig. 4c).

In vitro cytotoxicity of DOX-EM-NGs

Next, the *in vitro* cytotoxicity of nanogel against HeLa cells was evaluated by using the 3-(4,5-dimethylthiazol-2-yl)-2,5-diphenyltetrazolium bromide (MTT) assay. Both DOX-EM-NG and DOX-NG showed significantly enhanced cytotoxicity toward HeLa cells compared to free DOX solution upon 24-hour incubation (Fig. 5a). Notably, the cell *viability* of cells treated with DOX-EM-NG was much lower than that of those treated with DOX-NG, suggesting the better cell targeting ability of endosome membrane than the pure HA. The results were consistent with the cellular uptake studies measured above. Bare EM-NG did not exhibit significant cytotoxicity within the studied range of concentrations. In order to assess the capability of DOX-EM-NG to homotypically target cancer cells, the human lung adenocarcinoma epithelial (A549) cells, as a heterotypic cell line, were incubated with DOX-EM-NG or DOX-NG for 24 h. The results showed there was insignificant difference in

cell viability for DOX-EM-NG and DOX-NG (Fig. 5b), which further indicated that the enhanced binding effect was specifically associated with the membrane coating.

Conclusions

We have developed an innovative strategy utilizing endosome membrane-coated nanogels for enhanced delivery of anticancer drug. HA/SiO₂/Fe₃O₄ NPs encapsulating crosslinker and photo-initiator were confirmed to efficiently interact with endosomes by CLSM, and a subsequent *in situ* polymerization happened inside endosome, resulting in the endosome membrane coating HA nanogels. These EM-NGs containing magnetic nanocrystals were easily collected using a magnet after cell lysis. Through the western blotting analysis against endosome membrane specific protein (EEA1), the successful coating of endosome membrane was substantiated, and the endosome membrane shell could be removed *via* further lysis for long time. After loading with DOX, the resulting nanogel was demonstrated to efficiently target the source cancer cells through a specific homotypic affinity, which increased 1.5-fold in uptake efficiency compared to the bare HA NGs. Moreover, DOX-EM-NGs were able to deliver anticancer drug to source cancer cells with enhanced efficacy, while there were insignificant differences compared to DOX-NGs when treated toward non-source cancer cells.

Furthermore, stimuli-responsive moieties can be integrated with these EM-NGs to achieve controllable drug release⁴⁰. We will also evaluate *in vivo* targeting capability, antitumor efficacy and systemic toxicity of nanogel. This strategy provides guideline to develop endosome membrane-coated nanomedicine from primary tumors of patients for personalized anticancer treatments.

Supplementary Material

Refer to Web version on PubMed Central for supplementary material.

Acknowledgments

This work was supported by the grant from NC TraCS, NIH's Clinical and Translational Science Awards (CTSA, NIH grant 1UL1TR001111) at UNC-CH. We acknowledge the use of the Analytical Instrumentation Facility (AIF) at NC State, which is supported by the State of North Carolina and the National Science Foundation (NSF).

Notes and references

1. Mitragotri S, Anderson DG, Chen XY, Chow EK, Ho D, Kabanov AV, Karp JM, Kataoka K, Mirkin CA, Petrosko SH, Shi JJ, Stevens MM, Sun SH, Teoh S, Venkatraman SS, Xia YN, Wang ST, Gu Z, Xu CJ. *ACS Nano*. 2015; 9:6644–6654. [PubMed: 26115196]
2. Sarikaya M, Tamerler C, Jen AK-Y, Schulten K, Baneyx F. *Nat Mater*. 2003; 2:577–585. [PubMed: 12951599]
3. Gao W, Fang RH, Thamphiwatana S, Luk BT, Li J, Angsantikul P, Zhang Q, Hu C-MJ, Zhang L. *Nano Lett*. 2015; 15:1403–1409. [PubMed: 25615236]
4. Yoo J-W, Irvine DJ, Discher DE, Mitragotri S. *Nat Rev Drug Discov*. 2011; 10:521–535. [PubMed: 21720407]
5. Alvarez-Lorenzo C, Concheiro A. *Curr Opin Biotechnol*. 2013; 24:1167–1173. [PubMed: 23465754]
6. Balmert SC, Little SR. *Adv Mater*. 2012; 24:3757–3778. [PubMed: 22528985]

7. Copp JA, Fang RH, Luk BT, Hu C-MJ, Gao W, Zhang K, Zhang L. *Proc Natl Acad Sci.* 2014; 111:13481–13486. [PubMed: 25197051]
8. Hu C-MJ, Fang RH, Luk BT, Zhang L. *Nat Nanotechnol.* 2013; 8:933–938. [PubMed: 24292514]
9. Hu C-MJ, Fang RH, Copp J, Luk BT, Zhang L. *Nat Nanotechnol.* 2013; 8:336–340. [PubMed: 23584215]
10. Hu C-MJ, Zhang L, Aryal S, Cheung C, Fang RH, Zhang L. *Proc Natl Acad Sci.* 2011; 108:10980–10985. [PubMed: 21690347]
11. Fang RH, Hu C-MJ, Luk BT, Gao W, Copp JA, Tai Y, O'Connor DE, Zhang L. *Nano Lett.* 2014; 14:2181–2188. [PubMed: 24673373]
12. Hu Q, Qian C, Ye Y, Wang C, Gu Z. *Adv Mater.* 2015; 27:7043–7050. [PubMed: 26416431]
13. Scott CC, Vacca F, Gruenberg J. *Sem Cell Dev Biol.* 2014;2–10.
14. Seaman M. *Cell Mol Life Sci.* 2008; 65:2842–2858. [PubMed: 18726175]
15. Huotari J, Helenius A. *EMBO J.* 2011; 30:3481–3500. [PubMed: 21878991]
16. Caplan S, Naslavsky N, Hartnell LM, Lodge R, Polishchuk RS, Donaldson JG, Bonifacino JS. *EMBO J.* 2002; 21:2557–2567. [PubMed: 12032069]
17. Naslavsky N, Boehm M, Backlund PS, Caplan S. *Mol Biol Cell.* 2004; 15:2410–2422. [PubMed: 15020713]
18. Hettema EH, Lewis MJ, Black MW, Pelham HR. *EMBO J.* 2003; 22:548–557. [PubMed: 12554655]
19. Seaman MN. *J cell Sci.* 2012; 125:4693–4702. [PubMed: 23148298]
20. Gruenberg J, Howell KE. *Annu Rev Cell Biol.* 1989; 5:453–481. [PubMed: 2557061]
21. Foret L, Dawson JE, Villaseñor R, Collinet C, Deutsch A, Bruschi L, Zerial M, Kalaidzidis Y, Jülicher F. *Curr Biol.* 2012; 22:1381–1390. [PubMed: 22748321]
22. Chauhan VP, Martin JD, Liu H, Lacorre DA, Jain SR, Kozin SV, Stylianopoulos T, Mousa AS, Han X, Adstamongkonkul P. *Nat Commun.* 2013; 4
23. Khetan S, Guvendiren M, Legant WR, Cohen DM, Chen CS, Burdick JA. *Nat Mater.* 2013; 12:458–465. [PubMed: 23524375]
24. Toole BP. *Nat Rev Cancer.* 2004; 4:528–539. [PubMed: 15229478]
25. Culty M, Shizari M, Thompson EW, Underhill CB. *J Cell Physiol Suppl.* 1994; 160:275–286.
26. Swierczewska M, Choi KY, Mertz EL, Huang X, Zhang F, Zhu L, Yoon HY, Park JH, Bhirde A, Lee S. *Nano Lett.* 2012; 12:3613–3620. [PubMed: 22694219]
27. Zhao M, Liu Y, Hsieh RS, Wang N, Tai W, Joo K-I, Wang P, Gu Z, Tang Y. *J Am Chem Soc.* 2014; 136:15319–15325. [PubMed: 25289975]
28. Yan M, Du J, Gu Z, Liang M, Hu Y, Zhang W, Priceman S, Wu L, Zhou ZH, Liu Z. *Nat Nanotechnol.* 2010; 5:48–53. [PubMed: 19935648]
29. Mo R, Jiang T, DiSanto R, Tai W, Gu Z. *Nat Commun.* 2014; 5
30. Yu J, Zhang Y, Ye Y, DiSanto R, Sun W, Ranson D, Ligler FS, Buse JB, Gu Z. *Proc Natl Acad Sci.* 2015; 112:8260–8265. [PubMed: 26100900]
31. Gu Z, Yan M, Hu B, Joo K-I, Biswas A, Huang Y, Lu Y, Wang P, Tang Y. *Nano Lett.* 2009; 9:4533–4538. [PubMed: 19995089]
32. Jiang T, Mo R, Bellotti A, Zhou J, Gu Z. *Adv Funct Mater.* 2014; 24:2295–2304.
33. Lu AH, Salabas EeL, Schüth F. *Angew Chem Int Ed.* 2007; 46:1222–1244.
34. Kim J, Kim HS, Lee N, Kim T, Kim H, Yu T, Song IC, Moon WK, Hyeon T. *Angew Chem Int Ed.* 2008; 47:8438–8441.
35. Qian K, Ma Y, Wan J, Geng S, Li H, Fu Q, Peng X, Kan X, Zhou G, Liu W. *J Control Release.* 2015; 212:41–49. [PubMed: 26079186]
36. Wu W, Yao W, Wang X, Xie C, Zhang J, Jiang X. *Biomaterials.* 2015; 39:260–268. [PubMed: 25468376]
37. Jin Y-J, Termsarasab U, Ko S-H, Shim J-S, Chong S, Chung S-J, Shim C-K, Cho H-J, Kim D-D. *Pharm Res.* 2012; 29:3443–3454. [PubMed: 22886625]
38. Nukolova NV, Oberoi HS, Cohen SM, Kabanov AV, Bronich TK. *Biomaterials.* 2011; 32:5417–5426. [PubMed: 21536326]

39. Bertoli F, Davies GL, Monopoli MP, Moloney M, Gun'ko YK, Salvati A, Dawson KA. *Small*. 2014; 10:3307–3315. [PubMed: 24737750]
40. Lu Y, Sun W, Gu Z. *J Control Release*. 2014; 194:1–19. [PubMed: 25151983]

Author Manuscript

Author Manuscript

Author Manuscript

Author Manuscript

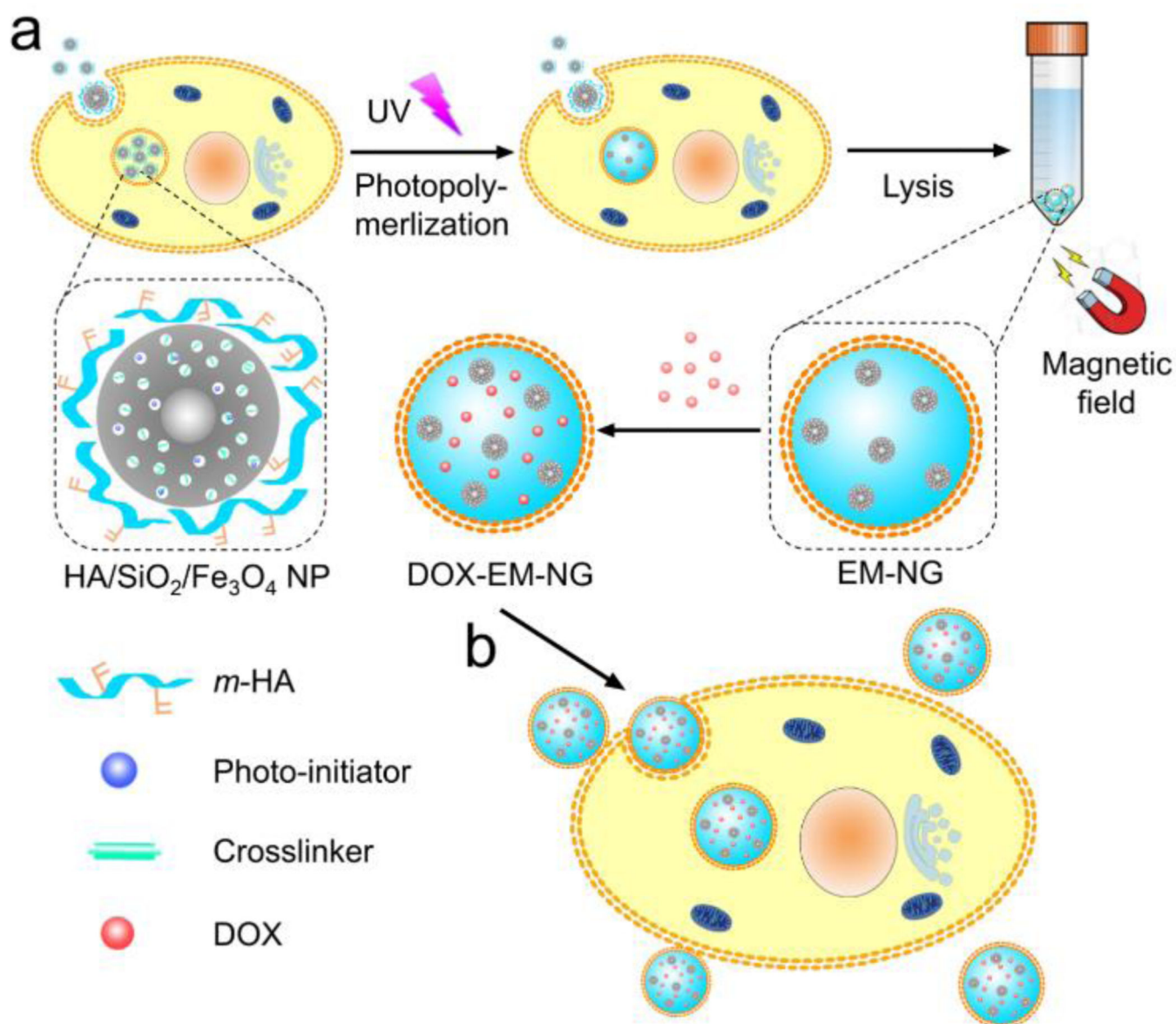


Fig. 1. Schematic of EM-NG for targeted drug delivery. (a) Preparation of EM-NG from source cancer cell. (b) DOX-loaded EM-NGs for targeted drug delivery.

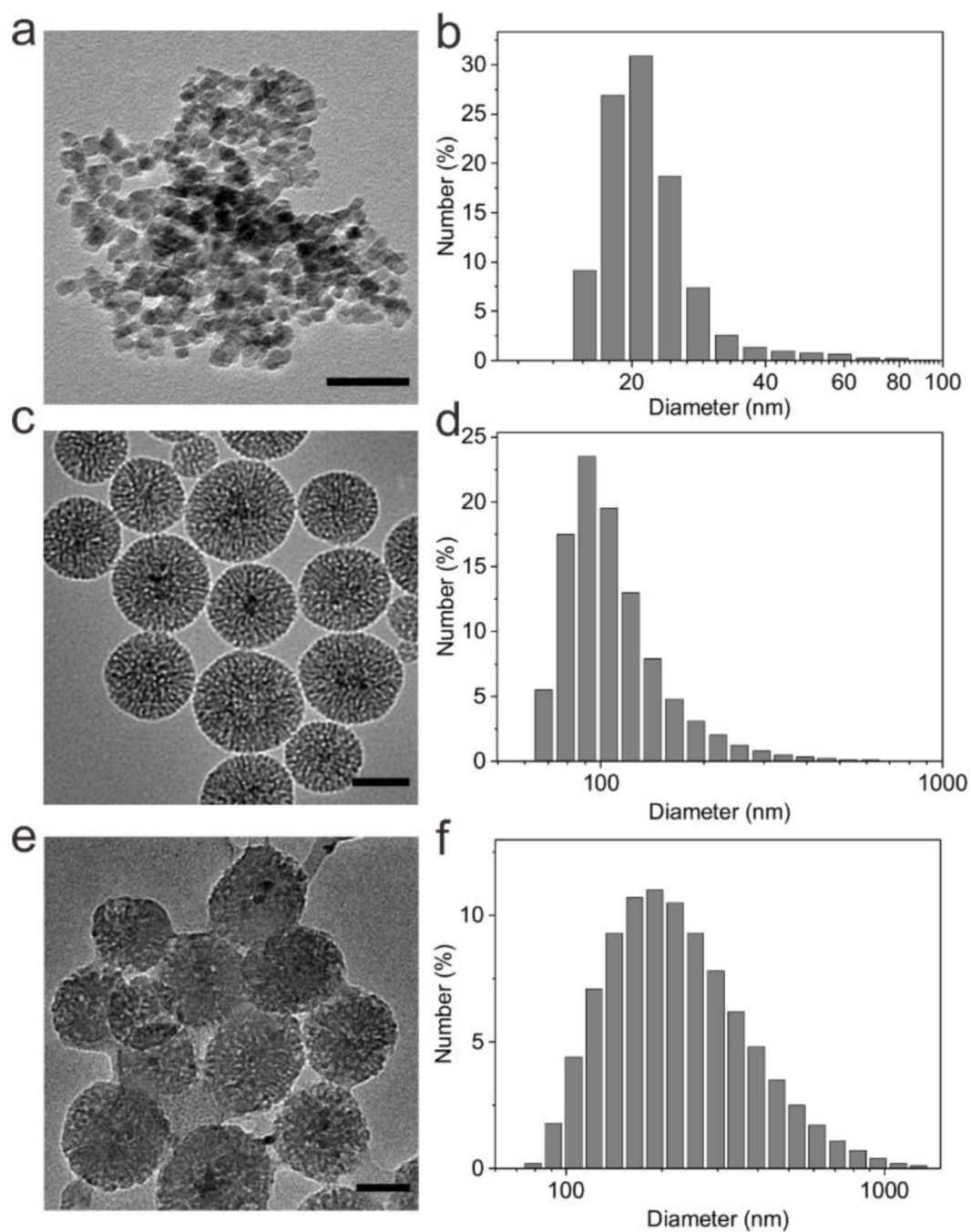


Fig. 2. Characterization of Fe₃O₄ nanocrystals, SiO₂/Fe₃O₄ NPs and HA/SiO₂/Fe₃O₄ NPs. (a) The TEM image and (b) size distribution of Fe₃O₄ nanocrystals. (Scale bar: 50 nm) (c) The TEM image and (d) size distribution of SiO₂/Fe₃O₄ NPs. (Scale bar: 50 nm) (e) The TEM image and (f) size distribution of HA/SiO₂/Fe₃O₄ NPs. (Scale bar: 50 nm)

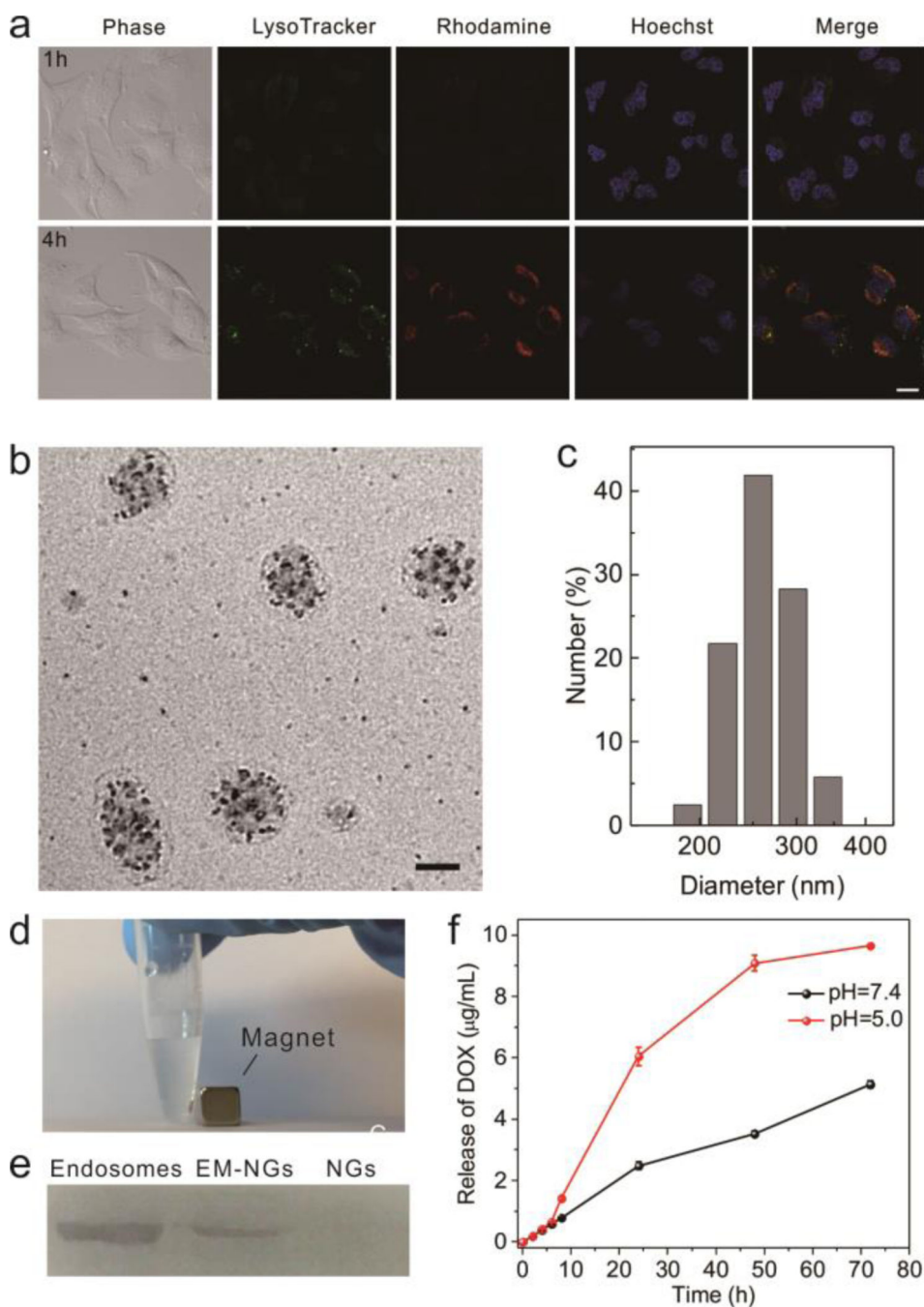


Fig. 3. Characterization of EM-NGs. (a) Intracellular trafficking of rhodamine labelled HA/SiO₂/Fe₃O₄ NPs on HeLa cell observed by CLSM. The late endo-lysosomes were stained by LysoTracker Green, and the nuclei were stained by Hoechst 33342. (Scale bar: 20 μm) (b) The TEM image and (c) size distribution of EM-NG. (Scale bar: 200 nm) (d) The photograph of EM-NGs collecting by magnetic field. (e) Western blotting analysis of endosomes, EM-NGs, and bare NGs against endosome membrane marker: the early

endosome antigen 1 (EEA1). (f) DOX release profiles of DOX-EM-NGs at pH 7.4 and 5.0, respectively.

Author Manuscript

Author Manuscript

Author Manuscript

Author Manuscript

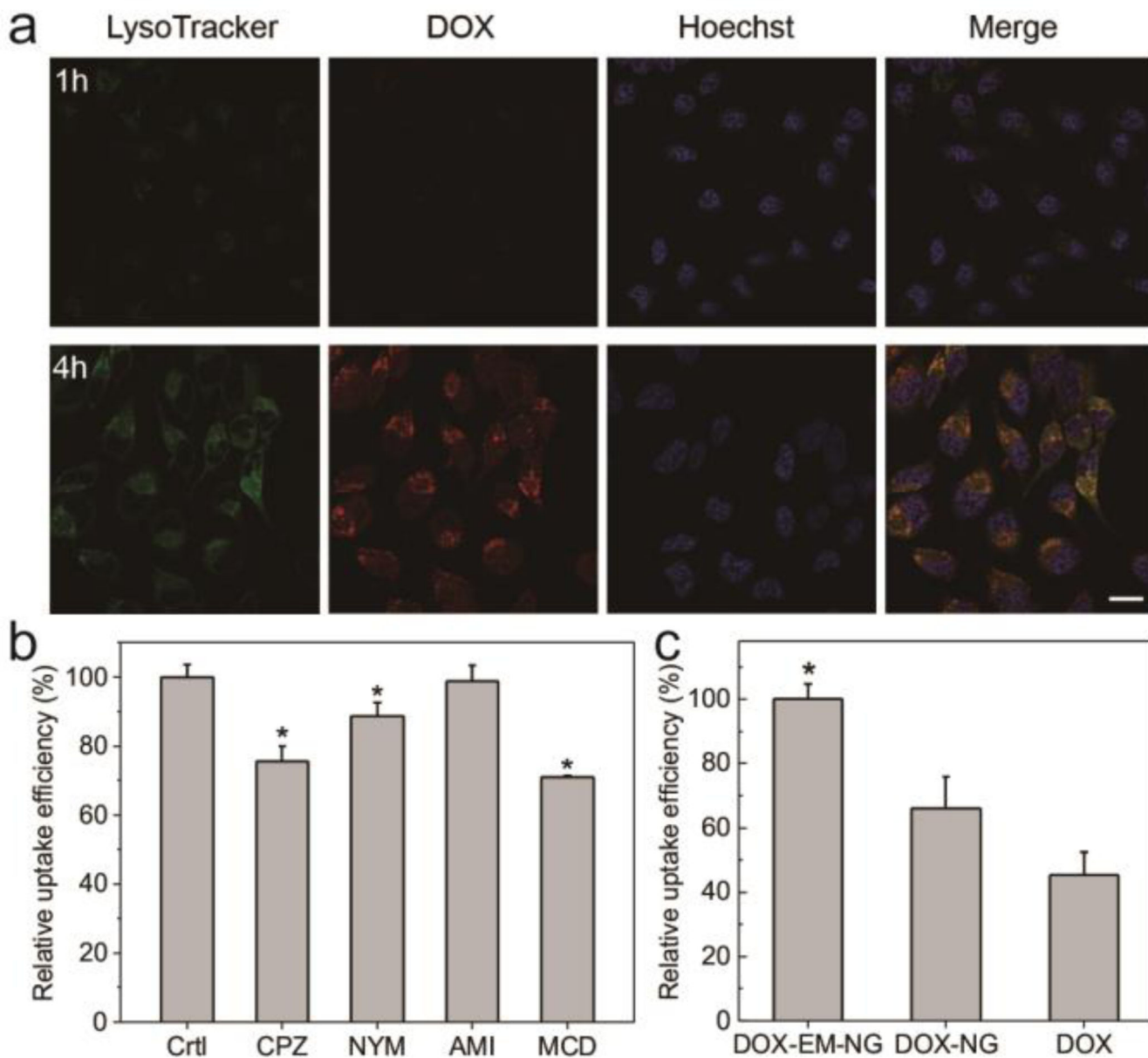


Fig. 4. *In vitro* delivery of DOX by EM-NG. (a) Intracellular trafficking of DOX-EM-NG observed by CLSM. The late endo-lysosomes were stained by LysoTracker Green, and the nuclei were stained by Hoechst 33342. (Scale bar: 20 μ m) (b) Investigation of cellular uptake mechanism. Relative uptake efficiency of DOX-EM-NG in the presence of various endocytosis inhibitors. Inhibitor of clathrin-mediated endocytosis: chlorpromazine (CPZ, 10 μ M); Inhibitor of caveolin-mediated endocytosis: nystatin (NYS, 25 μ g/mL); Inhibitor of macropinocytosis: amiloride (AMI, 1 mM); Inhibitor of lipid raft: methyl- β -cyclodextrin (MCD, 3 mM). * p <0.05 compared with control group. (c) Relative uptake efficiency of DOX-EM-NG, DOX-NG and free DOX on HeLa cells. * p <0.05 for treatment with DOX-EM-NG compared with DOX-NG and free DOX.

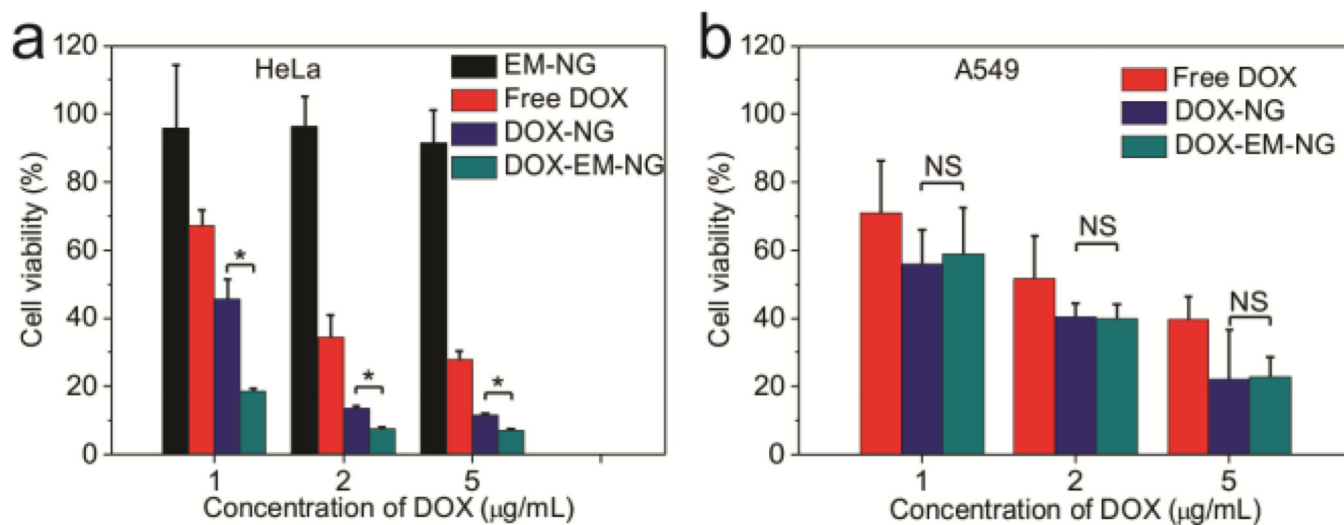


Fig. 5. *In vitro* cytotoxicity of DOX-EM-NG. (a) *In vitro* cytotoxicity of EM-NG, free DOX, DOX-NG and DOX-EM-NG towards HeLa cells after incubation for 24 h. (b) *In vitro* cytotoxicity of free DOX, DOX-NG and DOX-EM-NG towards A549 cells after incubation for 24 h. * $p < 0.05$, NS: not significant.